CORA Cork Open Research Archive
Cartlann Taighde Oscailte Chorcaí

Title	The role of length shift in assessing force and resistivity for optimized e-textile sensors
Authors	Gola, Gianmarco;Menolotto, Matteo;Demarchi, Danilo;O'Flynn, Brendan
Publication date	2025-07-18
Original Citation	Gola, G., Menolotto, M., Demarchi, D. and O'Flynn, B. (2025) 'The role of length shift in assessing force and resistivity for optimized e-textile sensors', 2025 IEEE International Instrumentation and Measurement Technology Conference (I2MTC), Chemnitz, Germany, 19-22 May 2025, pp. 1–6. https://doi.org/10.1109/I2MTC62753.2025.11079098
Type of publication	Conference item
Link to publisher's version	10.1109/I2MTC62753.2025.11079098
Rights	© 2025, IEEE. Personal use of this material is permitted. Permission from IEEE must be obtained for all other uses, in any current or future media, including reprinting/republishing this material for advertising or promotional purposes, creating new collective works, for resale or redistribution to servers or lists, or reuse of any copyrighted component of this work in other works.
Download date	2026-11-04 10:58:49
Item downloaded from	https://hdl.handle.net/10468/17783



University College Cork, Ireland
Coláiste na hOllscoile Corcaigh

The Role of Length Shift in Assessing Force and Resistivity for Optimized e-Textile Sensors

1^{st} Gianmarco Gola
Politecnico di Torino
Department of Electronics and Telecommunications
Turin, Italy
s317302@studenti.polito.it

2^{nd} Matteo Menolotto
Tyndall National Institute
University College Cork
Cork, Ireland
matteo.menolotto@tyndall.ie

3^{rd} Danilo Demarchi
Politecnico di Torino
Department of Electronics and Telecommunications
Turin, Italy
danilo.demarchi@polito.it

4^{th} Brendan O'Flynn
Tyndall National Institute
University College Cork
Cork, Ireland
brendan.oflynn@tyndall.ie

***Abstract*—Wearable sensors are becoming increasingly ubiquitous, revolutionizing the way we extract meaningful data from human subjects and compliant objects, such as soft and collaborative robots. E-textiles have emerged as a cost-effective solution that offers an optimal balance between sensitivity and mechanical compliance. However, current evaluations of e-textiles designed to transduce force into electrical signals often overlook the impact of natural length variations caused by mechanical stretching. This factor can compromise long-term accuracy, underscoring the need for a more comprehensive characterization approach. This work introduces and validates a novel assessment protocol that simultaneously tracks resistivity, force, and length variations in a conductive thread during different electro mechanical tests. The measurement system incorporates Wheatstone bridges as a front end to optimize the dynamic range of resistive readings and load cell signals, while employing an image processing approach to ensure precise length tracking. The results indicate a progressive increase in length after multiple stretch-recovery cycles, demonstrating how resistance and resting length evolve over repeated mechanical interactions. This approach facilitates the development of textile-based sensors and resistivity models that account for length variations during mechanical work, improving accuracy, and expanding the range of potential applications.**

***Index Terms*—Textile-based sensor, conductive fabric, e-textile, soft sensor**

I. Introduction

The integration of electronic textile (or e-textile) as sensors in wearable technology, agritech, and soft robotics has gained significant attention due to their flexibility, comfort, and ability to conform to flexible surfaces [1]–[3]. However, challenges remain in designing e-textiles that maintain consistent and reliable sensing capabilities under dynamic conditions [4], [5]. For soft robots, which frequently undergo complex deformation, there is a need for pressure sensors that can accurately capture the applied force without experiencing significant drift or loss in sensitivity [6]. E-textiles, specifically those woven with conductive threads, have emerged as promising candidates for creating pressure-sensitive surfaces [7]. Their compliancy and shapeless attributes make them ideal for applications in mechanically constrained environments where sensing precision and reliability are critical.

Various studies have focused on the electrical and mechanical properties of conductive yarns and fabrics, demonstrating their potential for deformation, pressure, and touch sensing. Prior research has typically assessed e-textile sensors under controlled conditions, measuring resistance changes in response to applied strain.

Pang et al. [8] characterized the electromechanical properties of a textile-based tactile sensor integrated with piezoresistive and triboelectric sensing layers on a cotton substrate. The sensor response to static and dynamic mechanical stimuli was tested using real-time physiological monitoring and machine learning-based texture perception, encountering mutual interference between sensing layers and challenges in maintaining mechanical robustness during prolonged use. A different approach was developed by Shekhar et al. [9], where elastic conductive yarns were created by plaiting, coiling, and twisting different mixture ratios of materials. The characterization focused on electrical conductivity, elasticity, and structural uniformity, identifying challenges in achieving simultaneous durability, elasticity, and low resistance, along with difficulties in adapting these yarns to existing textile manufacturing processes. Conductive wool yarns were manufactured by CNT impregnation and used to develop single layer pressure sensors in [10]. Characterization included resistance changes under pressure, SEM imaging, and durability tests over 20,000 cycles. Limitations included reduced flexibility and breathability due to the use of polyurethane films for encapsulation. A piezoresistive e-textile sensor using conductive polymer-coated

This work was carried out with the support of Research Ireland through the SFI Centre VistaMilk (21/RC/10303) and the Insight Centre for Data Analytics (SFI/12/RC/2289) and CONNECT, the Centre for Future Networks and Communications (13/RC/2077-2). This work is co-funded by the department scholarship from Politecnico di Torino. All work is co-funded under the European Regional Development Fund.

For the purpose of Open Access, the author has applied a CC BY public copyright licence to any Author Accepted

fabric was developed and characterized for shape sensing in soft continuum robots in [11]. Sensor hysteresis, sensitivity, and time response were analyzed, finding hysteresis-induced errors and challenges in maintaining consistent sensor behavior under prolonged cyclic deformation. In [12] elastic-conductive webbing made of Lycra and carbon-coated polyamide fibers was tested for tensile hysteresis and contact resistance during stretch-recovery cycles. Here, significant hysteresis losses and structural changes caused variability in resistance. In [13], 15 commercially available conductive yarns were evaluated for properties such as resistance to strain, mechanical durability, and electrical stability. Metal-based yarns exhibited high conductivity but poor mechanical properties, while coated yarns offered better mechanical compatibility but lower electrical performance. These approaches have laid the groundwork for the development of electronic textile sensors in applications such as health monitoring, human motion tracking, and soft robotics. However, despite advances in e-textile sensing, few studies have thoroughly characterized the behavior of conductive yarns under cyclical loading conditions where length and resistance changes are affected by elastic and plastic deformation of the fibers over time.

A significant challenge in applying conductive e-textiles as reliable sensors lies in understanding and modeling the impact of fiber relaxation and reorganization on resistance. Changes in thread length, resulting from internal fiber movement, introduce variability in resistance readings, complicating the accuracy and repeatability of the sensor. Most existing models for e-textile sensors do not account for these dynamic internal changes, leading to inconsistencies in resistance measurements under cyclical loading.

This study addresses these unresolved issues by focusing on the behavior of conductive threads under a constant applied force, assessing both resistance and length changes over multiple stretching cycles. Our approach deviates from traditional hysteresis testing, which typically holds thread length constant; instead, we allow for natural length relaxation and observe how these internal fiber adjustments influence the sensor resistance. Our hypothesis is that by accounting for fiber reorganization and length variation over repeated cycles of stretching under constant force, a more accurate and robust resistivity model can be developed for e-textile. This model will enable the creation of sensors that maintain consistent resistance responses, which is essential for their integration into collaborative soft robotic systems.

II. Materials and Methods

The conductive yarn selected for the study is Shieldex 117/17 (Shieldex, Bremen, Germany), a silver-plated polyamide/nylon filament (Fig. 1). Its high market availability and widespread use in numerous studies [14], [15] make it an ideal candidate for characterization in this investigation.

The measurement system consists of a stretching mechanism, an electrical front end for data acquisition, and a camera-based length detection module. A block diagram of the entire system is presented in Fig. 2, part B.

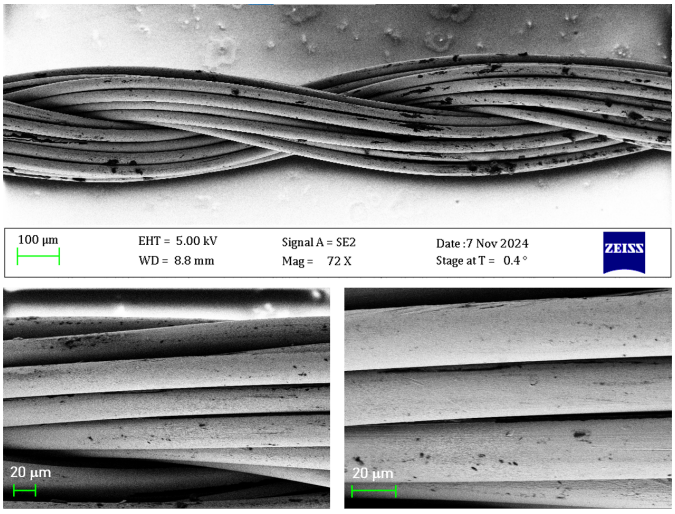


Fig. 1. SEM images of a representative conductive yarn (Shieldex 117/17), a Polyamide/Nylon 6.6 thread with 17 filaments coated in silver 99.9% pure.

A. Measurement Front End

The electronic front end used in this work, depicted in Fig. 2 part A, consists of a Wheatstone bridge connected to an instrumentation amplifier (AD623, Analog Devices, Wilmington, MA, USA). The Wheatstone bridge and the amplifier are powered by a bench power supply (Fluke, Everett, WA, USA) with supply voltages of $V_{CC1} = 3\,\mathrm{V}$ and $V_{CC2} = 4.5\,\mathrm{V}$, respectively. The Wheatstone bridge is constructed using high-precision resistors with a temperature coefficient of $2.5\ ppm/^{\circ}\mathrm{C}$ to ensure stability. The resistors are configured as $R_1 = R_2 = 1\,\mathrm{k\Omega} \pm 0.05\%$ and $R_3 = R_4 = 250\,\Omega \pm 0.05\%$. These values are selected to minimize tolerance-induced errors while maintaining an acceptable current level for the fabric under test R_x serially connected to R_4 on the Wheatstone bridge (typically in the range of tens of ohms). By using resistors with different values, the bridge gain, defined as $A = R_1/R_3 = R_2/R_4$, increased. This reduces bridge sensitivity $S = V_{CC1} \cdot A/(A+1)^2$, but also decreases nonlinearity, as it is inversely proportional to the bridge gain, resulting in improved linearity in the measurement.

The output of the Wheatstone bridge is then processed by the AD623 instrumentation amplifier, powered at $3\,\mathrm{V}$. The gain resistor, R_g, was set to $10\,\mathrm{k\Omega} \pm 1\%$, setting the amplifier to a gain of $G = 11.0 \pm 0.1$. A reference voltage $V_{ref} = 1.07\,\mathrm{V}$ established using a voltage divider ensured that the signal remained within the operational range of the amplifier, avoiding saturation. In this setup, the upper limit of the signal was $4.5\,\mathrm{V}$ and the lower limit was $0\,\mathrm{V}$. The designed front end can measure the fabric resistance within a range of $0\,\Omega$ to $94\,\Omega$, corresponding to an output voltage range of approximately $1\,\mathrm{V}$ to $3\,\mathrm{V}$. This ensured compatibility with the ADC used, which had a maximum allowable input voltage of $3.1\,\mathrm{V}$. Data acquisition was performed using the Portenta H7 board (Arduino, Monza, Italy), which features a 16 bit ADC, while the data processing was performed by a

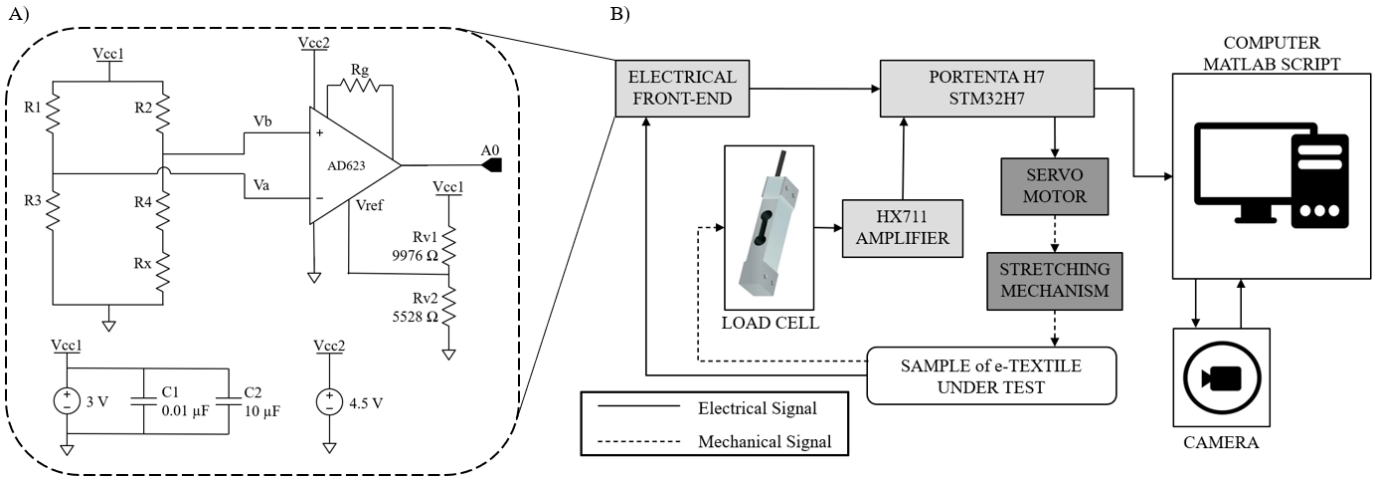


Fig. 2. A) Electrical front end: The custom Wheatstone bridge comprises four resistances: $R_1 = R_2 = 1\,\mathrm{k\Omega} \pm 0.05\%$, $R_3 = R_4 = 250\,\Omega \pm 0.05\%$; where R_x represent the e-textile yarn under test. The bridge output is connected to an instrumentation amplifier AD623, with a gain resistance $R_g = 10\,\mathrm{k\Omega} \pm 1\%$ and a reference voltage $V_{ref} = 1.07\,\mathrm{V}$, defined by a voltage partition between $R_{v1} = 10\,\mathrm{k\Omega} \pm 1\%$ and $R_{v2} = 5.6\,\mathrm{k\Omega} \pm 5\%$. B) Measurement system: The Portenta H7 (STM32H7 microcontroller) receives data from the front end and the HX711 amplifier, which processes load cell signals. The Portenta H7 controls a continuous rotation servo motor for the stretching mechanism, which cyclically stretches and relaxes the sample. Data is transmitted to a computer, where MATLAB scripts generate datasets and control a webcam for timed image acquisition.

MATLAB (MathWorks, Natick, Massachusetts, USA) script running on a Windows PC.

B. Stretching Mechanism

The stretching mechanism consists of a continuous rotation servo motor (Parallax Inc., CA, USA) that applies torque to a reduction gearbox, driving a slide block fixed on a guide rail to convert the rotary motion into linear displacement (Fig. 3 part B). The gearbox includes six gears: the transmission gear, directly mounted on the servo motor axis, a ratchet gear with a selection mechanism (pawl) to divide the full rotation into 17 incremental steps, three intermediate reduction gears, and a traction gear that moves the slide block. The overall reduction ratio from the transmission gear to the traction gear is approximately $455 : 1$, resulting in a linear motion of approximately $0.48\,\mathrm{mm}$ per step of the ratchet gear (equivalent to approximately $2.4\,\mathrm{mm}$ for a complete rotation of the transmission gear). The entire gearbox was custom designed and 3D manufactured in PLA (polylactic acid).

The conductive thread under test is secured to two hooks by loops at its ends. One hook is connected to a load cell ($1\,\mathrm{kg}$ range, accuracy $\pm 0.02\%$, relative linearity error $\pm 0.02\%$) that measures the force applied during fabric tension, while the other hook is attached to the slide block (Fig. 3 part C). The load cell output is amplified by an HX711 amplifier (AVIA Semiconductors, Xiamen, P. R. China), which transmits the force data to the Portenta H7 board. The servo motor, which drives the slide block through a gearbox, is controlled by the Portenta H7 board. This setup enables precise regulation of the fabric's tension, both based on the servo's rotation angle and dynamically adjusted using force feedback from the load cell.

C. Length Assessment

For each test, the length of the sample (L), defined as the distance between the two probes (Fig. 3 part C), was determined by recording a video using a camera (Logitech, Lausanne, Switzerland) and selecting frames that correspond to the end of each servo motor movement (either the end of a stretch or release). An image processing workflow was then implemented to extract the location of the hooks in pixels on the probes $P1$ and $P2$, which had been coated with green paint for easier detection, and the squares of a reference checkerboard ($5\,\mathrm{mm}$ square size), used as a scale reference, as shown in Fig. 3, part C. To identify the precise frames marking the end of the servo motor movement, force data were analyzed to detect local maxima (example in Fig. 4, column 1). Combining the information of start time, sampling frequency, and frame rate of the video, the exact frames were extracted and converted to images. These images were processed by first converting them to grayscale and then to binary (black and white), simplifying the identification of the reference checkerboard. The grid provided a pixel-to-millimeter conversion factor, as the number of pixels corresponding to a square. To detect the positions of the green-painted hooks on the probes, the original RGB images were converted to HSV (hue, saturation, value) color space. The Hue channel provided optimal contrast for segmenting the green regions. The centroids of the identified green areas were defined as the positions of $P1$ and $P2$, and the Euclidean distance between these centroids was calculated in pixels. Finally, the pixel distance was converted to millimeters using the checkerboard reference, yielding the actual sample length.

D. Resistance-Force-Length Measurement Protocol

The characterization focuses on three fundamental parameters: relative resistance, applied force, and relative length.

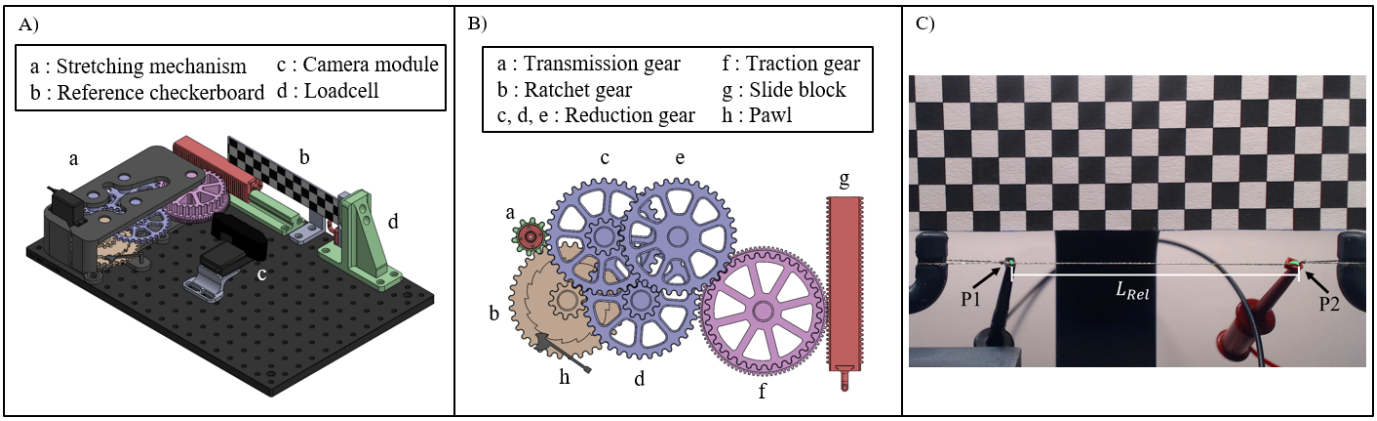


Fig. 3. A) CAD model of the measurement setup. B) Stretching Mechanism composed by: servo motor with correspondent transmission gear (a) of 10 teeth, ratchet gear (b) with 17 : 5 gear ratio and 17 steps on it and correspondent pawl (h), three intermediate reduction gears (c, d, e) with 17 : 5 gear ratio, the traction gear (f) and a slide block (g) with teeth on edges for shift movement. C) Sample view during the measurement: sample resistance was detected across two hook clips $P1$ and $P2$ connected trough two loops at two hooks, probes color was green to detect easily their position using the camera and detecting correspondent length of sample (L_{Rel}) exploiting the reference checkerboard above the sample.

Resistance and force were measured using the front end circuit and the load cell, while length was obtained using the camera-based approach mentioned above.

1) Static Analysis: This set of measurements aims to understand how resistance and force change as a function of strain, and to understand the relaxation behavior of the thread. For this test, the length of the sample was increased by one step of the ratchet gear, corresponding to $0.48\,\mathrm{mm}$, until reaching 105% of its original length. This process was performed on samples with three different starting lengths (L_0): $5\,\mathrm{cm}$, $7.5\,\mathrm{cm}$, and $10\,\mathrm{cm}$. To ensure that the sample was under tension, the length was increased until the load cell was detected $1.5\,\mathrm{N}$. After 1 minute of relaxation, the Portenta board activated the servo motor to increase the length of the sample by one step of the ratchet gear with a speed of $0.21\mathrm{mm/s}$ followed by $15\,\mathrm{s}$ of relaxation. This process was carried out for a number of steps necessary to reach roughly 105% of the initial length: 8 *steps* for $5\,\mathrm{cm}$, 10 *steps* for $7.5\,\mathrm{cm}$, and 13 *steps* for $10\,\mathrm{cm}$. The frequency of resistance and force data collection was 1.7Hz, while the length was detected every time the sample was stretched. The temperature and humidity of the room was monitored throughout the experiment, recording stable values of $T = 23\pm2\,^{\circ}\mathrm{C}$ and $H = 50\pm5\%$, respectively. For each of the three different sample groups (different L_0), 12 different samples were used to account for intrinsic variability of the e-textiles. This number was obtained considering the desired margin of error (E) and the confidence level (CL) as: $E = 0.6\,\Omega$ and $CL = 95\%$. In a preliminary test, 10 threads of $5\,\mathrm{cm}\pm0.5\,\mathrm{cm}$ were stretched until the applied force was $1.5\,\mathrm{N}$, acquiring at least 10 samples of resistance. From this procedure, the standard deviation (σ) of the samples was calculated ($\sigma = 1.0383\,\Omega$), and using Eq. 1, the final sample size was evaluated $n = 12$.

$$n = \frac{(Z \cdot \sigma)^2}{E^2} \tag{1}$$

2) Hysteresis Effect: Hysteresis measurements play a crucial role in evaluating the performance and reliability of e-textiles for dynamic applications, such as their integration into sensors for robotic handling systems. In these applications, the ability to repeatedly grab and release objects at a defined frequency depends on the material's ability to maintain consistent mechanical and electrical properties under cyclic loading and unloading conditions.

The hysteresis test was performed on e-textile samples with a length of $5\,\mathrm{cm}$, reflecting the expected dimensions of a future wearable sensor. The test involved stretching the sample to a force of $1.5\,\mathrm{N}$, holding this position for a waiting time of $t_w = 5\,\mathrm{s}$, further stretching it to $4.5\,\mathrm{N}$, maintaining the force for the same duration, and then relaxing it back to $1.5\,\mathrm{N}$. The upper force limit was determined by a break test conducted on three samples of the same length. The average breaking force was found to be $9\,\mathrm{N}$. To avoid significant damage during cyclic stretching, 50% of the breaking force ($4.5\,\mathrm{N}$) was chosen as a safe and effective upper limit, balancing the need for a wide dynamic range with the durability of the thread.

This cycle was repeated 20 times and the length was detected every time the sample reached $1.5\,\mathrm{N}$ and $4.5\,\mathrm{N}$. The stretching and relaxation of the sample occurred at the same speed as the static test. This procedure was also performed with waiting times of $t_w = 10\,\mathrm{s}$ and $t_w = 30\,\mathrm{s}$. For higher reliability, the hysteresis measurement for each t_w was performed for three different samples, and to detect variation after this procedure, the same sample was retested the day after and 2 days after with the same procedure and parameters.

III. Results and Discussion

During the static assessment, the length of the samples was increased by $0.48\,\mathrm{mm}$ for each step required to achieve approximately 105% of the initial L_0. The selected e-textile exhibited linear behavior, with a variation of $2.5\,\Omega$ observed in the sample population (Fig. 4, column 1). No significant differences were observed in the relationship between resistance

and length variation between the three groups of different L_0. Similarly, the variation in force sensitivity remained consistent throughout the population (Fig. 4, columns 2 and 3). The resistance of the e-textile increased with applied force, demonstrating a high degree of linearity $R^2 = 0.9843$. Notably, a force relaxation is observed after each stretch, as evident from the force peaks in Fig. 4, column 1. Although fiber relaxation leads to an increase in thread length and a decrease in applied force, resistance values remain unchanged for the durations t_w selected in this test.

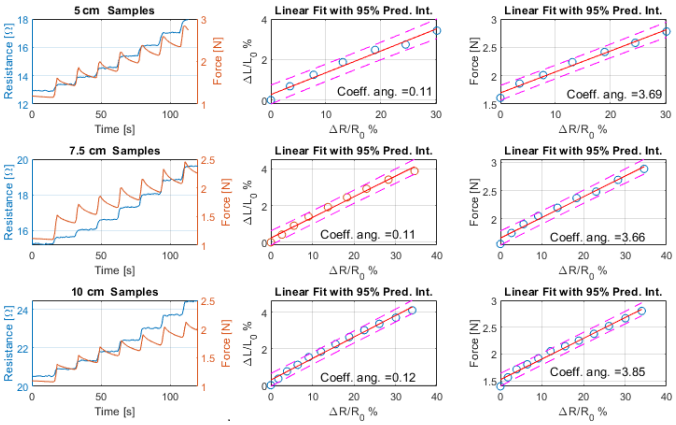


Fig. 4. Results from the static test: The first column shows the force increment due to controlled stretching and the corresponding resistance increase for sample populations with initial lengths of 5 cm (row 1), 7.5 cm (row 2), and 10 cm (row 3). The second column presents the relative variation of $\Delta L/L_0$ compared to $\Delta R/R_0$, while the last column illustrates the force variation relative to $\Delta R/R_0$.

In the hysteresis test, the minimum and maximum applied forces were kept constant to investigate the effect of initial variation in yarn length which is assumed to be caused by stretching and subsequent reorganization of the fibers on resistivity changes. Fig. 5 illustrates a gradual increase in both resting length L_{Rel} and maximum stretch length L_{Str} over time. This contributes to the observed resistance variation shown in Fig. 6, even with a consistent applied force. Table I summarizes the slope of the increase in L_{Rel} and L_{Str} during stretch-release cycles of varying durations (5, 10 and 30 s) for three consecutive days using the same set of three samples. In general, the slope decreases over repeated cycles and days, indicating a stabilization or accommodation in the initial structure of the yarn, resulting in greater dimensional stability.

The observed length variations (Fig. 7) are influenced by the intrinsic behavior of the textile, as evidenced by static tests. However, the resistance shift shown in Fig. 6 can also be partially attributed to the gradual degradation of the silver coating on the fibers, a natural consequence of the mechanical stress imposed by repeated hysteresis cycles [16].

IV. Conclusions

This study highlights the importance of a comprehensive characterization protocol for conductive e-textiles to improve

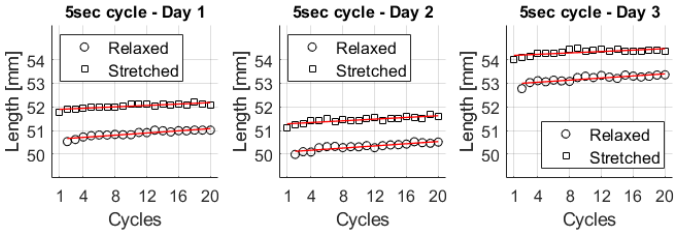


Fig. 5. Results from the hysteresis test: example of the increase in L_{Rel} and L_{Str} observed during 5 s stretch-release cycles over three consecutive days (measurements temporally proceed from left to right).

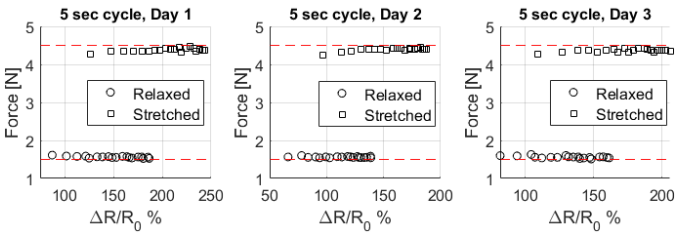


Fig. 6. Example of the shift in $\Delta R/R_0$ observed during the hysteresis test. Despite maintaining a constant force, $\Delta R/R_0$ progressively increases over successive cycles (measurements temporally proceed from left to right).

their application in wearable sensors and soft robotics. By integrating resistivity, force, and length measurements, we demonstrated that mechanical stretching leads to progressive fiber reorganization, which significantly affects the resistivity and dimensional stability of the textile over time. The static tests revealed a linear relationship between the applied force and the resistance, showing a high degree of predictability between samples of different lengths. However, hysteresis tests revealed dynamic behaviors, such as gradual increases in resting and maximum lengths (L_{Rel} and L_{Str}), and resistance changes over successive cycles, even under consistent force application. These findings underscore the necessity of considering fiber relaxation and structural changes when designing resistivity models for e-textiles.

Taking these factors into account, the proposed characterization protocol enables the development of more accurate and robust sensor models. Such sensors could maintain long-term reliability and precision, making them ideal for dynamic applications such as collaborative robotics, where consistent sensing performance under cyclic mechanical stress is critical. This work sets the foundation for future developments in textile-based sensors, emphasizing the need for multi-parameter assessments to optimize performance and expand their potential applications.

A. Limitations

Although this study provides valuable insights into the behavior of conductive e-textiles under cyclic mechanical stress, several limitations need to be acknowledged. The first flaw is represented by the limited dynamic range of the electrical front end, which had an upper limit for readable resistance equal to 94 Ω. This limitation is not feasible when a long sample is used

TABLE I
HYSTERESIS MEASUREMENT DATA: CHANGES IN L_0 AND THE SLOPE OF THE FITTED LINE REPRESENTING THE VARIATION IN L.

Parameter	t_w **= 5 seconds**				t_w **= 10 seconds**				t_w **= 30 seconds**			
	Day 1	***Day 2***	***Day 3***	***Mean***	***Day 1***	***Day 2***	***Day 3***	***Mean***	***Day 1***	***Day 2***	***Day 3***	***Mean***
L_0 (mm)	48.2	47.9	50.4	48.8	49.4	49.2	51.7	50.1	49.5	49.3	51.9	50.2
Slope of L_{Rel}	0.023	0.023	0.022	0.023	0.018	0.015	0.016	0.016	0.020	0.016	0.013	0.016
Slope of L_{Str}	0.015	0.018	0.015	0.016	0.012	0.013	0.011	0.012	0.012	0.011	0.008	0.010

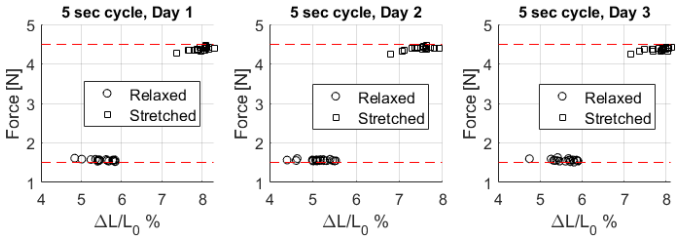


Fig. 7. Example of the shift in $\Delta L/L_0$ observed during the hysteresis test. Both L_{Rel} and L_{Str} are subjected to a stretch during the successive cycles (measurements temporally proceed from left to right).

or a higher number of cycles on hysteresis measurements is performed because it would become impossible to detect resistance after a certain stimulus. Another limitation encountered was about camera resolution. The resolution of the camera combined with the length detection algorithm creates an error in the length detection. The resolution used in this work was 576p; consequentially, the error in length detection was $\pm 0.1\,\mathrm{mm}$.

Furthermore, the study focuses on a single type of conductive yarn (Shieldex 117/17), limiting the generalizability of the findings to other e-textile materials with different compositions or structural properties. Mechanical stress imposed on the yarn, such as stretching, is applied in a unidirectional manner, which may not represent complex deformations experienced in real-world applications, such as soft robotics or wearable systems.

B. Future Works

To achieve a more comprehensive understanding of the behavior of conductive e-textiles, future work should explore hysteresis measurements with extended waiting times ($1\,\mathrm{h}$ and $24\,\mathrm{h}$) to better evaluate the changes in fiber relaxation and resistivity over prolonged intervals. Furthermore, conducting hysteresis tests with a higher number of cycles, such as 50 or 200, would provide a more detailed assessment of material fatigue and degradation over time.

To optimize the experimental efficiency, the setup could be modified to allow parallel testing of multiple threads, allowing a broader dataset to be collected within the same timeframe. Future investigations should also consider testing different e-textile materials and applying multidirectional mechanical stress to better simulate the complex conditions encountered in practical applications. These enhancements would contribute to a 360-degree overview of the material's behavior and further improve the design and reliability of textile-based sensors for dynamic environments.

ACKNOWLEDGMENT

We thank Alida Russo for her help with the acquisition of the SEM images.

REFERENCES

[1] Islam, G.N., Ali, A. and Collie, S., 2020. Textile sensors for wearable applications: A comprehensive review. Cellulose, 27, pp.6103-6131.
[2] Sanchez, V., Walsh, C.J. and Wood, R.J., 2021. Textile technology for soft robotic and autonomous garments. Advanced functional materials, 31(6), p.2008278.
[3] Fu, C., Xia, Z., Hurren, C., Nilghaz, A. and Wang, X., 2022. Textiles in soft robots: Current progress and future trends. Biosensors and Bioelectronics, 196, p.113690.
[4] Martinez, R.V., 2023. Wearables, E-textiles, and Soft Robotics for Personalized Medicine. In Springer Handbook of Automation (pp. 1265-1287). Cham: Springer International Publishing.
[5] Du, K., Lin, R., Yin, L., Ho, J.S., Wang, J. and Lim, C.T., 2022. Electronic textiles for energy, sensing, and communication. IScience, 25(5).
[6] Shih, B., Christianson, C., Gillespie, K., Lee, S., Mayeda, J., Huo, Z. and Tolley, M.T., 2019. Design considerations for 3D printed, soft, multimaterial resistive sensors for soft robotics. Frontiers in Robotics and AI, 6, p.30.
[7] Galeta, E.V., Nada, A.A., Ahmed, S.M., Parque, V. and El-Hussieny, H., 2024. A Soft e-Textile Sensor for Enhanced Deep Learning-based Shape Sensing of Soft Continuum Robots. arXiv preprint arXiv:2404.12627.
[8] Pang, Y., Xu, X., Chen, S., Fang, Y., Shi, X., Deng, Y., Wang, Z.L. and Cao, C., 2022. Skin-inspired textile-based tactile sensors enable multifunctional sensing of wearables and soft robots. Nano Energy, 96, p.107137.
[9] Shekhar, R., Choudhry, N.A., Islam, S., Ahnood, A., Pirogova, E. and Troynikov, O., 2023. A novel elastic conductive yarn for smart textile applications. Advanced Engineering Materials, 25(22), p.2300572.
[10] Kim, G., Vu, C.C. and Kim, J., 2020. Single-layer pressure textile sensors with woven conductive yarn circuit. Applied Sciences, 10(8), p.2877.
[11] Galeta, E.V., Ahmed, S., Parque, V. and El-Hussieny, H., 2023, September. Design and characterization of an e-textile sensor for shape sensing of soft continuum robots. In 2023 62nd Annual Conference of the Society of Instrument and Control Engineers (SICE) (pp. 1110-1115). IEEE.
[12] Shyr, T.W., Shie, J.W. and Jhuang, Y.E., 2011. The effect of tensile hysteresis and contact resistance on the performance of strain-resistant elastic-conductive webbing. Sensors, 11(2), pp.1693-1705.
[13] Chen, Y., Hart, J., Suh, M., Mathur, K. and Yin, R., 2023. Electromechanical Characterization of Commercial Conductive Yarns for E-Textiles. Textiles, 3(3), pp.294-306.
[14] Micus, S., Padani, L., Haupt, M. and Gresser, G.T., 2021. Textile-based coils for inductive wireless power transmission. Applied Sciences, 11(9), p.4309.
[15] Martínez-Estrada, M., Moradi, B., Fernández-Garcia, R. and Gil, I., 2019. Impact of conductive yarns on an embroidery textile moisture sensor. Sensors, 19(5), p.1004.
[16] Xue, P., Tao, X.M. and Tsang, H.Y., 2007. In situ SEM studies on strain sensing mechanisms of PPy-coated electrically conducting fabrics. Applied surface science, 253(7), pp.3387-3392.